Nonsteady Flame Spreading in Two-Dimensional Ducts

Malladi V. Subbaiah*
California Institute of Technology, Pasadena, California

Nonsteady behavior of a flame stabilized at the center of a two-dimensional duct is studied using an integral technique. An exact representation of the irrotational flow field upstream of the flame is obtained by utilizing a suitable distribution of sources on the duct axis. Time-dependent solutions exhibit traveling wave patterns with significant amplification along the flame region. These solutions enable the calculation of the acoustic transmission and reflection properties of the flame region.

I. Introduction

THE control and elimination of combustion instability in systems of practical interest and the rational interpretation of subscale experiments require an understanding of the fundamental mechanism. In many instances response of the combustion processes to local pressure and velocity fluctuations is an important factor that feeds considerable energy into the system to sustain the oscillations. When the frequency is less than a few hundred hertz, the chemical reaction time delay is relatively unimportant, rather, the fluid mechanical adjustments of the flame region play the dominant role governing the detailed response of the system.

As a result of fast chemical kinetics, flame fronts are usually very thin compared to length scales associated with combustion devices of practical interest. Therefore, in problems where detailed calculations of flame structure are not important, one often considers the flame front as a surface of discontinuity separating the cold fuel oxidizer mixture and hot combustion products. The flowfields on either side of the flame front are matched by relations analogous to the jump conditions across the shock discontinuities.

Nonsteady behavior of a flame stabilized at the center of a two-dimensional duct is studied as a specific but typical example of the low-frequency behavior. Steady-state flame spreading of the confined premixed flames in two-dimensional ducts, stabilized by bluff body flame holders, attracted the attention of several early research workers.[1] Scurlock,[2] Tsien,[3] Ball,[4] Fabri et al.,[5] and Iida[6] studied the problem analytically, while Williams et al.,[7] Thurston,[8] and Wright and Zukoski[9] investigated experimentally.

Scurlock[2] was the first to investigate steady flowfield and flame spreading from idealized cylindrical flame holders in a two-dimensional duct. He obtained a numerical solution for the flame shape and velocity profile in the region downstream of the flame. Incompressible flow with a uniform velocity profile in the unburned region and uniform static pressure across any cross section were assumed. Tsien[3] provided a simpler treatment of the above problem with assumed uniform velocity in the cold region and linear velocity distribution in the hot region, as suggested by Scurlock's results. He further extended his calculations to include compressibility effects and found that for large approach Mach number or heat release, the flame did not reach the channel wall and the input fuel mixture was not completely burned. Tsien also calculated vorticity produced by the flame in terms of fluid velocity and streamline curvature immediately upstream of the flame. Zukoski[10] showed that the flame shape is relatively insensitive to the assumed velocity profile in the burned region. However, the maximum velocity in the hot region will obviously depend on the assumed profile. Fabri et al.[5] and Iida[6] linearized the equations of motion for small flame speeds and obtained an integral equation for stream function, which was solved by successive integration. The assumption of uniform velocity in the unburned region does not provide accurate initial conditions for these calculations.

In the above calculations, momentum transfer in the direction normal to the duct walls was ignored. Validity of such calculations is restricted to very low flame speeds in comparison to the approaching fluid velocity. Also, in the above quasi-one-dimensional approaches, flame shape and flowfield as a function of the downstream distance from the flame holder are not readily available. Additional approximation on the velocity component at the flame, in a direction perpendicular to the channel axis, has to be made for an accurate description of the flame shape. Ball[4] made a two-dimensional calculation for the steady flame shape and flowfield in a two-dimensional duct by solving incompressible, inviscid, laminar flow equations of motion by a relaxation method. Such a calculation is not restricted to very low flame speeds and shows the effect of pressure field set up by the flame.

Although the steady flame spreading and flowfield of stabilized two-dimensional flames were under investigation for a considerable period, the nonsteady behavior of such flames did not receive the same attention. However, the analogous problem of stability of plane flames, known as Landau instability, was extensively studied. Landau[11] showed that laminar plane flames with constant flame speed were unstable to disturbances of all wavelengths and interpreted the result as the onset of flame-generated turbulence. Subsequent analyses by Markstein[12] and Istratov and Librovich[13] and experiments by Peterson and Emmons[14] were aimed at explaining the experimentally observed stable laminar flames by incorporating the effects of flame curvature, heat conduction, and viscosity on the flame propagation. Blackshear[15] studied the temporal instability of the stabilized flame subjected to transverse velocity disturbances. The flame was modeled as an impermeable interface separating two parallel streams (burned and unburned regions) with local velocity profiles as assumed by Tsien. The results indicate that the interface is neutrally stable to symmetric disturbances and unstable to antisymmetric disturbances, when the velocity profile is uniform in the unburned region and triangular in the burned region.

Presented as Paper 81-1348 at the AIAA/SAE/ASME 17th Joint Propulsion Conference, Colorado Springs, Colo., July 27-29, 1981; submitted Feb. 19, 1982; revision received Feb. 14, 1983.

*Post-Doctoral Research Fellow, Presently, Senior Aeronautical and Mechanical Engineer, Failure Analysis Associates, Palo Alto, Calif. Member AIAA.

Marble and Candel[16] were the first to identify the nonsteady fluid mechanical response of stabilized flames as a possible source of the low-frequency oscillations observed in large combustors like the utility boilers and aircraft afterburners. They analyzed the nonsteady behavior of a flame stabilized by a flame holder of finite size in a two-dimensional duct, subjected to external acoustic disturbances. In a recent extension to the nonsteady flame model, Le Chatelier and Candel[17] included the effects of compressibility and variations in duct geometry. The present investigation is a continuation of the work initiated by Marble and Candel.[16]

Nonsteady behavior of a flame stabilized in a two-dimensional duct is analyzed in this paper. The problem is formulated in the next section using an integral technique in which the governing equations are integrated across the duct to obtain certain integral relations for the averaged flow variables. The flowfields on either side of the flame sheet are matched by appropriate matching conditions. Flow through the flame surface causes the integral relations to explicitly involve the fluid velocities at the flame. To provide this information an independent description of the irrotational flowfield upstream of the flame is required. An exact representation of the upstream region is obtained in the third section by utilizing a suitable distribution of nonsteady sources on the duct axis.

The integral relations developed in Sec. II are analyzed by a perturbation technique, in which the dominant order solution represents the steady flame development. The steady flame configuration is perturbed by an acoustic wave incident on the flame region. The time-dependent counterpart of the integral relations describes the ensuing nonsteady flowfields. The flame perturbation exhibits a traveling wave pattern with considerable amplification along the flame zone.

Acoustic reflection and transmission coefficients of the flame region can be obtained utilizing the time-dependent flame calculations. The response spectra exhibit active responses at certain well-defined frequencies. The analysis enables one to couple the flame region with the acoustics of the combustion system in which the stabilized flame is situated.[18]

II. General Formulation of a Stabilized Flame

A. Analytical Description of a Nonsteady Stabilized Flame

Consider a flame, stabilized by a flame holder of half-width η_0, in a two-dimensional parallel duct of width 2ℓ, as shown in Fig. 1. The flame region is modeled as a surface of discontinuity separating the cold fuel/oxidizer mixture, region 1, and hot combustion products, region 2. Let $\eta(x,t)$ be the distance of the flame sheet from the centerline of the duct, the x axis. A combustible mixture of fuel and oxidizer approaches the flame region with a uniform velocity U_0 far upstream. Let $p(x,y,t)$ and $\rho(x,y,t)$ be the pressure and density, and $u(x,y,t)$ and $v(x,y,t)$ be the velocity components parallel and normal to the duct axis. The variables are indicated by subscript *1* in region 1, upstream of the flame, and by subscript *2* in region 2, downstream of the flame.

Neglecting gravitational and viscous effects, the flowfields in regions 1 and 2 are governed by the following equations.

In region 1, continuity equation

$$\frac{\partial \rho_1}{\partial t}+\frac{\partial}{\partial x}(\rho_1 u_1)+\frac{\partial}{\partial y}(\rho_1 v_1)=0 \tag{1}$$

Momentum equations

$$\frac{\partial}{\partial t}(\rho_1 u_1)+\frac{\partial}{\partial x}(\rho_1 u_1^2)+\frac{\partial}{\partial y}(\rho_1 u_1 v_1)=-\frac{\partial p_1}{\partial x} \tag{2}$$

$$\frac{\partial}{\partial t}(\rho_1 v_1)+\frac{\partial}{\partial x}(\rho_1 u_1 v_1)+\frac{\partial}{\partial y}(\rho_1 v_1^2)=-\frac{\partial p_1}{\partial y} \tag{3}$$

Neglecting heat conduction also, the energy equation can be written in the form

$$\frac{1}{p_1}\frac{\mathrm{D}_1 p_1}{\mathrm{D}t}-\frac{\gamma}{\rho_1}\frac{\mathrm{D}_1 \rho_1}{\mathrm{D}t}=\frac{1}{C_v}\frac{\mathrm{D}_1 s_1}{\mathrm{D}t}=0 \tag{4}$$

where γ is the ratio of specific heats, C_p/C_v, and s_1 is the specific entropy, and

$$\frac{\mathrm{D}_1}{\mathrm{D}t}\equiv\frac{\partial}{\partial t}+u_1\frac{\partial}{\partial x}+v_1\frac{\partial}{\partial y}$$

The above equation states that the entropy remains constant, following the fluid. We assume the flowfield far upstream to be irrotational with uniform velocity U_0 and of uniform entropy. Consequently, flow in region 1 can be considered as irrotational and hence isentropic.

A similar set of equations is written for region 2, using subscript *2* for the dependent variables. However, the flowfield in region 2 is, in general, rotational as a result of the entropy produced by the flame. This aspect of vorticity production by the flame will be considered later in some detail.

The above flowfields in regions 1 and 2 are matched across the flame sheet by mass and momentum conservation relations, analogous to the jump conditions across shock discontinuities in compressible flows.

Conservation of mass gives

$$\rho_1 w_1=\rho_2 w_2 \tag{5}$$

where w_1 and w_2 are the flame speeds. w_1/U_0 and w_2/U_0 are assumed to be constant.

The momentum equation normal to the flame surface gives

$$p_1+\rho_1 w_1^2=p_2+\rho_2 w_2^2 \tag{6}$$

Since the static pressure is continuous along the flame sheet, the tangential momentum equation implies that the tangential velocity is continuous across the flame surface.

$$u_1\cos\Theta+\left(v_1-\frac{\partial\eta}{\partial t}\right)\sin\Theta=u_2\cos\Theta+\left(v_2-\frac{\partial\eta}{\partial t}\right)\sin\Theta \tag{7}$$

Also, we must have the flame sheet and flowfields deform in a consistent manner. In the present context we have fixed propagation speeds normal to the flame and the kinematic conditions at the flame surface imply that the normal velocity of the fluid, relative to the flame surface, is equal to the corresponding flame speed.

$$\frac{\partial\eta}{\partial t}\cos\Theta+u_1\sin\Theta-v_1\cos\Theta=w_1 \tag{8}$$

$$\frac{\partial\eta}{\partial t}\cos\Theta+u_2\sin\Theta-v_2\cos\Theta=w_2 \tag{9}$$

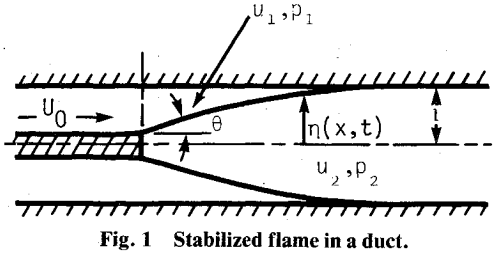

Fig. 1 Stabilized flame in a duct.

Assuming specific heat to be constant, the energy equation at the flame surface can be written in the quasisteady approximation as

$$\rho_1 w_1\left[C_p T_1+\frac{1}{2}\left\{w_1^2+\left(u_1\cos\Theta+v_1\sin\Theta-\frac{\partial\eta}{\partial t}\sin\Theta\right)^2\right\}+\Sigma_1\right]$$
$$=\rho_2 w_2\left[C_p T_2+\frac{1}{2}\left\{w_2^2+\left(u_2\cos\Theta+v_2\sin\Theta-\frac{\partial\eta}{\partial t}\sin\Theta\right)^2\right\}+\Sigma_2\right] \tag{10}$$

where Σ_1 and Σ_2 are the energies of formation per unit mass for the gas in regions 1 and 2, respectively. T_1 and T_2 are the gas temperatures in the two regions. For combustion processes of practical interest, increase in sensible enthalpy, $(\Sigma_1-\Sigma_2)$, is much larger than the changes in kinetic energy. Therefore, we can approximate Eq. (10) by

$$C_p T_1+\Sigma_1 \approx C_p T_2+\Sigma_2 \tag{11}$$

From Eq. (6),

$$p_2/p_1=1-\gamma(w_1/c_1)^2(\rho_1/\rho_2-1) \tag{12}$$

and depends on the square of the Mach number based on the flame speed, which is considered to be small. Consequently, we can approximate,

$$T_2/T_1\approx\rho_1/\rho_2\approx 1+(\Sigma_1-\Sigma_2)/(C_p T_1) \tag{13}$$

However, it is important to consider the pressure change across the flame in the momentum balance and in the determination of the flame shape.

B. Development of the Integral Relations

We wish to investigate the nonsteady behavior of the stabilized flame when subjected to external acoustic disturbances. Consistent with the approximation in Eq. (13), we can consider the flowfields in regions 1 and 2 as incompressible. There is, of course, a large density change across the flame as given by Eq. (13). The pressure changes associated with the acoustic disturbance and the changes in the gas velocities are so small that they do not influence the combustion process significantly.

To describe the flowfields in regions 1 and 2 by an integral technique, continuity and momentum equations are integrated with respect to y, between the flame and the channel wall. In region 1, upstream of the flame, the integration is carried out from $y=\eta(x,t)$ to $y=\ell$ as shown below.

With the incompressible flow approximation discussed earlier, Eq. (1) becomes

$$\int_{\eta(x,t)}^{\ell}\frac{\partial u_1}{\partial x}\,dy+\int_{\eta(x,t)}^{\ell}\frac{\partial v_1}{\partial y}\,dy=0$$

We use the boundary condition at the solid wall,

$$v_1(x,\ell,t)=0 \tag{14}$$

and obtain

$$\frac{\partial}{\partial x}\int_{\eta}^{\ell}u_1\,dy+u_1(x,\eta,t)\frac{\partial\eta}{\partial x}-v_1(x,\eta,t)=0 \tag{15}$$

Defining a mean axial velocity

$$\bar{u}_1(x,t)=\frac{1}{[\ell-\eta(x,t)]}\int_{\eta(x,t)}^{\ell}u_1\,dy \tag{16}$$

and using the kinematic condition Eq. (8), we get from Eq. (15)

$$\frac{\partial}{\partial t}(\ell-\eta)+\frac{\partial}{\partial x}[(\ell-\eta)\bar{u}_1]+w_1\sec\Theta=0 \tag{17}$$

A similar integration of the other governing equations results in the following equations for the integral variables.

$$\frac{\partial}{\partial t}[(\ell-\eta)\bar{u}_1]+\frac{\partial}{\partial x}[(\ell-\eta)\bar{u}_1^2]+\frac{(\ell-\eta)}{\rho_1}\frac{\partial\bar{p}_1}{\partial x}$$
$$+u_1(x,\eta,t)\,w_1\sec\Theta=0 \tag{18}$$

$$\frac{\partial\eta}{\partial t}+\frac{\partial}{\partial x}(\eta\bar{u}_2)-w_2\sec\Theta=0 \tag{19}$$

$$\frac{\partial}{\partial t}(\eta\bar{u}_2)+\frac{\partial}{\partial x}(\eta\bar{u}_2^2)+\frac{\eta}{\rho_2}\frac{\partial\bar{p}_2}{\partial x}-u_2(x,\eta,t)\,w_2\sec\Theta=0 \tag{20}$$

The equations of motion in the y direction assure that the variations of static pressure across the two regions are small. In arriving at the above equations, the following assumptions were made.

$$p_1(x,\eta,t)=\bar{p}_1(x,t) \qquad p_2(x,\eta,t)=\bar{p}_2(x,t)$$

$$\int_{\eta}^{\ell}(u_1-\bar{u}_1)^2\,dy=0 \qquad \int_{\eta}^{\ell}(u_2-\bar{u}_2)^2\,dy=0$$

These approximations are similar to the ones usually made for shallow water wave calculations, wherein the normal acceleration of the fluid is neglected. In the present context, these assumptions are strictly valid only for the case of slender flames, subjected to low-frequency disturbances. Stabilized flames observed in the laboratory (Williams, et al.[7] and Wright and Zukoski[9]) and in typical technological applications like afterburners (Zukoski[10]) usually meet this criterion.

The above integral relations and matching conditions explicitly involve the local fluid velocities at the flame surface in both of the regions. To complete the formulation we have to independently estimate at least one velocity component at $y=\eta(x,t)$. This is to be expected because we have fluid propagation through the flame and because local momentum transfer at the flame should play an important role in the flame development. An exact solution for the irrotational flowfield upstream of the flame is presented in Sec. III. An approximation for $u_1(x,\eta,t)$ will be developed from this exact solution.

The above system of equations is studied using a perturbation technique in which the zeroth-order steady-state solution is perturbed by an acoustic wave incident on the flame region.

III. Steady-State Flame Calculations

A. Approximate Analysis for the Steady-State Flame Development

Let the mean axial velocity, pressure, and density be denoted by $\bar{u}_1^{(0)}(x)$, $\bar{p}_1^{(0)}(x)$, and ρ_1 in region 1, and by $\bar{u}_2^{(0)}(x)$, $\bar{p}_2^{(0)}(x)$, and ρ_2 in region 2. Let w_1 and w_2 be the fixed burning velocities, as in Sec. II, and

$$\frac{d\eta^{(0)}}{dx}\ll 1 \tag{21}$$

In region 1, mass conservation gives

$$\frac{d}{dx}[(\ell-\eta^{(0)})\bar{u}_1^{(0)}]=-w_1 \tag{22}$$

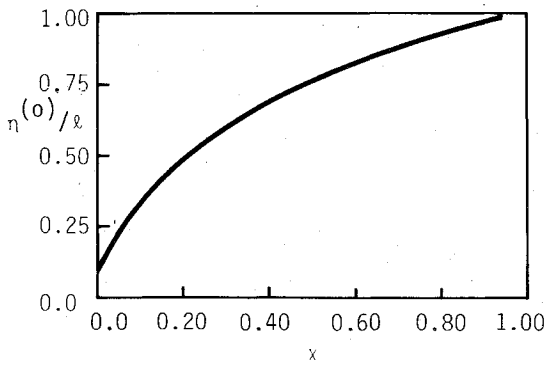

Fig. 2 Steady flame shape, $\lambda = 4.5$.

With the assumed uniform approach velocity U_0 far upstream, the flowfield in region 1 is irrotational, and we use the Bernoulli equation upstream of the flame and write

$$\frac{\bar{p}_1^{(0)}}{\rho_1 U_0^2} + \frac{1}{2}\left[\frac{\bar{u}_1^{(0)}}{U_0}\right]^2 = \frac{1}{\gamma M_0^2} + \frac{1}{2} \tag{23}$$

where p_0 is the static pressure far upstream, $\gamma = C_p/C_v$ and M_0 is the approach Mach number. In region 2, mass conservation gives

$$\frac{\mathrm{d}}{\mathrm{d}x}(\eta^{(0)}\bar{u}_2^{(0)}) = w_2 \tag{24}$$

Next, we utilize the overall momentum conservation equation to get

$$\rho_1 U_0^2 \ell + p_0 \ell = \rho_1 (\bar{u}_1^{(0)})^2 (\ell - \eta^{(0)}) + \bar{p}_1^{(0)} (\ell - \eta^{(0)}) + \rho_2 (\bar{u}_2^{(0)})^2 \eta^{(0)} + \bar{p}_2^{(0)} \eta^{(0)} \tag{25}$$

Consistent with the approximation Eq. (21), we assume that the streamlines are nearly parallel to the duct axis and treat the static pressure to be uniform in regions 1 and 2. However, normal momentum balance across the flame [Eq. (6)] gives

$$\bar{p}_1^{(0)} - \bar{p}_2^{(0)} = (\lambda - 1)\rho_1 w_1^2 \tag{26}$$

Integrating Eq. (22), and defining

$$\chi = (x/\ell)(w_1/U_0) \tag{27}$$

we get

$$\frac{\bar{u}_1^{(0)}}{U_0} = (A - \chi)\Big/\left(1 - \frac{\eta^{(0)}}{\ell}\right) \tag{28}$$

Similarly, Eq. (24) gives

$$\frac{\bar{u}_2^{(0)}}{U_0} = (B + \lambda\chi)\Big/\left(\frac{\eta^{(0)}}{\ell}\right) \tag{29}$$

where $\lambda = \rho_1/\rho_2$ and A and B are constants of integration.

At the flame holder of half-width η_0 at $x = 0$, we assume the mean axial velocities in the two streams to be equal and write the mass conservation equation to get

$$\frac{\bar{u}_1^{(0)}(0)}{U_0} = \frac{\bar{u}_2^{(0)}(0)}{U_0} = 1\Big/\left(1 - \frac{\eta_0}{\ell} + \frac{1}{\lambda}\frac{\eta_0}{\ell}\right) \tag{30}$$

Calculations were also made using different values [e.g., $\bar{u}_2^{(0)}(0) = 0$] for the mean axial velocity in region 2 at the flame holder. The results indicate that the effect is very localized near the flame holder and that the overall flame development is not appreciably altered. The above choice gives a flame shape with a positive slope at the flame holder. Hence, in Eqs. (28) and (29),

$$A = \left(1 - \frac{\eta_0}{\ell}\right)\Big/\left(1 - \frac{\eta_0}{\ell} + \frac{1}{\lambda}\frac{\eta_0}{\ell}\right) \tag{31}$$

$$B = \frac{\eta_0}{\ell}\Big/\left(1 - \frac{\eta_0}{\ell} + \frac{1}{\lambda}\frac{\eta_0}{\ell}\right) \tag{32}$$

We substitute $\bar{u}_1^{(0)}$, $\bar{u}_2^{(0)}$, and $\bar{p}_1^{(0)}$ into the overall momentum conservation Eq. (25) and obtain

$$\left(\frac{1}{2} - \frac{\eta^{(0)}}{\ell}\right)\left[\frac{A - \chi}{1 - \eta^{(0)}/\ell}\right]^2 + \frac{1}{\lambda}\frac{\eta^{(0)}}{\ell}\left[\frac{B + \lambda\chi}{\eta^{(0)}/\ell}\right]^2 - (\lambda - 1)[w_1/U_0]^2(\eta^{(0)}/\ell) = 1/2 \tag{33}$$

which is cubic in $\eta^{(0)}$ and quadratic in χ.

For simplicity Eq. (33) is solved for $\chi(\eta^{(0)})$ to obtain the flame shape $\eta^{(0)}(x)$ implicitly. A typical flame shape for $\lambda = 4.5$ is shown in Fig. 2.

Mean axial velocities and pressure are obtained from Eqs. (28), (29), and (23). Distribution of $\bar{u}_1^{(0)}$ and $\bar{u}_2^{(0)}$ for the above flame configuration is shown in Fig. 3 and exhibits an approximately linear increase with the axial distance from the flame holder.

It can at once be observed from Eqs. (33), (28), and (29) that the flame shape and flow variables exhibit a similarity representation for all flame speeds $w_1/U_0 \ll 1$, with $\chi = (x/\ell)(w_1/U_0)$ as the similarity variable.

B. An Exact Representation for the Steady-State Flowfield Upstream of a Stabilized Flame

As was discussed in Sec. II, the flowfield upstream of the flame is irrotational and can also be approximated as incompressible. Consequently, there exists a unique scalar potential $\phi(x,y)$ such that

$$\frac{\partial^2\phi}{\partial x^2} + \frac{\partial^2\phi}{\partial y^2} = 0 \tag{34}$$

and

$$u_1^{(0)}(x,y) = \frac{\partial\phi}{\partial x} \tag{35}$$

$$v_1^{(0)}(x,y) = \frac{\partial\phi}{\partial y} \tag{36}$$

For the present calculation, let us consider the flame $\eta^{(0)}(x)$ to be stabilized by an idealized flame holder of negligible thickness, located at $x = 0$. The kinematic condition [Eq. (8)] at the flame surface in region 1, specialized to steady flow, can be written as

$$u_1^{(0)}(x,\eta^{(0)})\frac{\mathrm{d}\eta^{(0)}}{\mathrm{d}x} = v_1^{(0)} + w_1 \sec\Theta^{(0)} \tag{37}$$

which can be written, using Eqs. (35) and (36), as

$$\left[\left(\frac{\partial\phi}{\partial x}\right)^2 - w_1^2\right]\left[\frac{\mathrm{d}\eta^{(0)}}{\mathrm{d}x}\right]^2 - 2\frac{\partial\phi\partial\phi\mathrm{d}\eta^{(0)}}{\partial x\partial y\mathrm{d}x} + \left(\frac{\partial\phi}{\partial y}\right)^2 - w_1^2 = 0 \tag{38}$$

With a suitable description of $\phi(x,y)$, the above equation can be integrated to obtain $\eta^{(0)}(x)$, subjected to the initial condition $\eta^{(0)} = 0$ at $x = x_0$, where x_0 is obtained from the

equation

$$u_1^{(0)}(x_0,0)=\frac{\partial\phi}{\partial x}(x_0,0)=w_1 \tag{39}$$

The flame shape obtained from the approximate calculation of the previous section and the results of Ball,[4] lead us to model the flowfield, upstream of the flame, by a source distribution located on the axis of the duct in the flame region.

The complex velocity $w(x+iy)$ due to a uniform source distribution of strength $(4\ell U_0\beta^{(0)})/L$ per unit length extending from $x=0$ to $x=L$ on the axis of a two-dimensional channel of width 2ℓ can be written as

$$\frac{w}{U_0}(x+iy)=\frac{u_1^{(0)}}{U_0}-i\frac{v_1^{(0)}}{U_0}$$
$$=2\frac{\beta^{(0)}}{\pi}\frac{\ell}{L}\log_e\left[\frac{\sinh(\pi z/2\ell)}{\sinh[\pi(z-L)/2\ell]}\right]+(1+\beta^{(0)}) \tag{40}$$

In the above equation uniform flow is added such that the approach velocity far upstream is U_0. From the analysis of Sec. III.A, we take $\ell/L\approx w_1/U_0$, where L is the length of the flame region. We also choose the total source strength such that $u_1^{(0)}(L)$ is approximately equal to the value obtained from the previous section.

In the results presented here, to generate acceptable flame envelopes, the source strengths selected are $\beta^{(0)}=1.0$ for $\lambda=4.5$ and $\beta^{(0)}=0.44$ for $\lambda=2.25$. Typical flame envelopes for $w_1/U_0=0.1$, 0.2, and 0.4 are shown in Fig. 4 for $\lambda=4.5$. Flame shape and streamlines upstream of the flame for $\lambda=4.5$ are shown in Fig. 5 for $w_1/U_0=0.4$. This flowfield is compared with the results of Ball[4] and the agreement is very good. The above potential solution, of course, does not describe the flowfield downstream of the flame.

In the early stages of flame spreading, the axial velocity $u_1(x,y)$ is strongly non-uniform over the cross section. To complete the formulation in Sec. II, we intend to obtain an approximation for $[u_1^{(0)}(x,\eta^{(0)})]/\bar{u}_1^{(0)}(x)$, where $\bar{u}_1^{(0)}$ is the mean axial velocity. Distributions of $[u_1^{(0)}(x,\eta^{(0)})]/\bar{u}_1^{(0)}(x)$ and $[v_1^{(0)}(x,\eta^{(0)})]/\bar{u}_1^{(0)}(x)$ are shown in Fig. 6 for the above stabilized flame. In the integral relations, we approximate $u_1^{(0)}(x,\eta^{(0)})$ by

$$\left[1-\frac{u_1^{(0)}(x,\eta^{(0)})}{\bar{u}_1^{(0)}(x)}\right]\left(1+\frac{\delta x}{\ell}\right)=1 \tag{41}$$

where $\delta=1/0.014$.

The above approximation, together with the matching conditions [Eqs. (5-9)] provide all the velocity components at the flame surface for the steady-state flame development.

C. Numerical Solution of the Steady-State Integral Relations

The integral relations [Eqs. (17-20)] are analyzed by a perturbation technique. The perturbation scheme consists of the dominant order solution representing the steady-state flame development, together with time-dependent perturbations caused by the imposed disturbances. Let $\eta^{(0)}(x)$ represent the steady-state flame shape and $\bar{p}_1^{(0)}(x)$, $\bar{p}_2^{(0)}(x)$, and $\bar{u}_1^{(0)}(x)$, $\bar{u}_2^{(0)}(x)$ denote the average static pressures and velocities in the two regions. The dependent variables in the integral relations are decomposed as

$$\eta(x,t)=\eta^{(0)}(x)+\eta^{(1)}(x,t)$$
$$\bar{u}_1(x,t)=\bar{u}_1^{(0)}(x)+\bar{u}_1^{(1)}(x,t)\ \text{ etc.} \tag{42}$$

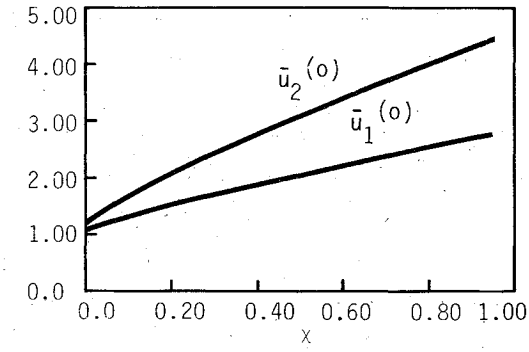

Fig. 3 Average axial velocities, $\lambda=4.5$.

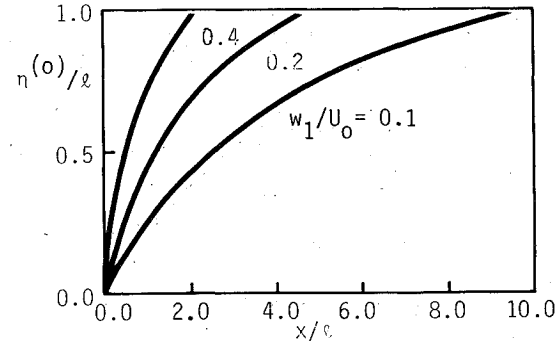

Fig. 4 Steady flame envelopes, $\lambda=4.5$, $\beta^{(0)}=1.0$.

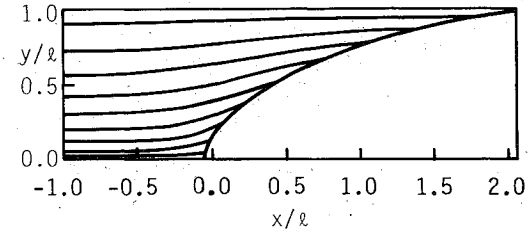

Fig. 5 Streamlines upstream of the flame, $\lambda=4.5$, $w_1/U_0=0.4$.

and

$$|\eta^{(1)}(x,t)|\ll|\eta^{(0)}(x)|\ \text{ etc.} \tag{43}$$

Substituting Eq. (42) into the integral relations Eqs. (17-20), we get for the steady-state flame development

$$\frac{d}{dx}[(\ell-\eta^{(0)})\bar{u}_1^{(0)}]+w_1\sec\Theta^{(0)}=0 \tag{44}$$

$$\bar{u}_1^{(0)}\frac{d\bar{u}_1^{(0)}}{dx}+\frac{1}{\rho_1}\frac{d\bar{p}_1^{(0)}}{dx}+\frac{[u_1^{(0)}(x,\eta^{(0)})-\bar{u}_1^{(0)}]}{\ell-\eta^{(0)}}w_1\sec\Theta^{(0)}=0 \tag{45}$$

$$\frac{d}{dx}(\eta^{(0)}\bar{u}_2^{(0)})-w_2\sec\Theta^{(0)}=0 \tag{46}$$

$$\bar{u}_2^{(0)}\frac{d\bar{u}_2^{(0)}}{dx}+\frac{1}{\rho_2}\frac{d\bar{p}_2^{(0)}}{dx}+\frac{[\bar{u}_2^{(0)}-u_2^{(0)}(x,\eta^{(0)})]}{\eta^{(0)}}w_2\sec\Theta^{(0)}=0 \tag{47}$$

In Eqs. (45) and (47), $u_1^{(0)}(x,\eta^{(0)})$ is obtained from the approximation Eq. (41) and from the matching conditions at the

flame,

$$u_2^{(0)}(x,\eta^{(0)}) = u_1^{(0)}(x,\eta^{(0)}) + w_1(\lambda-1)\sin\Theta^{(0)} \tag{48}$$

Further, the pressure fields in the two regions are related through the normal momentum balance [Eq. (6)].

We assume a small flame holder of half-width η_0 located at $x=0$ and consider as in Sec. III.A, $\tilde{u}_1^{(0)}(0) = \tilde{u}_2^{(0)}(0)$ at $x=0$. This gives the initial conditions for the steady problem as

$$\eta^{(0)}(0) = \eta_0 \tag{49}$$

$$\tilde{u}_1^{(0)}(0) = \tilde{u}_2^{(0)}(0) = U_0\ell/(\ell - \eta_0 + \eta_0/\lambda) \tag{50}$$

$$\tilde{p}_1^{(0)}(0) = p_0 + (\rho_1/2)[U_0^2 - (\tilde{u}_1^{(0)}(0))^2] \tag{51}$$

The above system of differential equations is integrated numerically to obtain $\eta^{(0)}(x)$, $\tilde{u}_1^{(0)}(x)$, $\tilde{u}_2^{(0)}(x)$, and $\tilde{p}_1^{(0)}(x)$.

Steady flame envelopes for the three flame speeds, $w_1/U_0 = 0.1$, 0.2, and 0.4, and for an approach Mach number, $M_0 = U_0/C_1 = 0.2$, are shown in Fig. 7 for $\lambda = 4.5$. The flame shapes are not very sensitive to changes in the approach Mach number for low Mach numbers. The flame envelopes and flowfields are in good agreement with the results of the approximate analysis of Sec. III.A and the exact representation of the previous section.

D. Vorticity Production by the Flame

With the assumed approach conditions far upstream, the flowfield upstream of the flame surface is irrotational. However, the downstream flow is, in general, rotational due to the vorticity produced by the flame. In this section, we wish to obtain an expression for this vorticity production in terms of the upstream flow variables and the flame shape.

For the steady flame development, we can write the matching conditions at the flame surface, $y = \eta^{(0)}(x)$, as

$$u_1^{(0)}(x,\eta^{(0)})\frac{d\eta^{(0)}}{dx} = v_1^{(0)}(x,\eta^{(0)}) + w_1\sec\Theta^{(0)} \tag{52}$$

$$u_2^{(0)}(x,\eta^{(0)})\frac{d\eta^{(0)}}{dx} = v_2^{(0)}(x,\eta^{(0)}) + w_2\sec\Theta^{(0)} \tag{53}$$

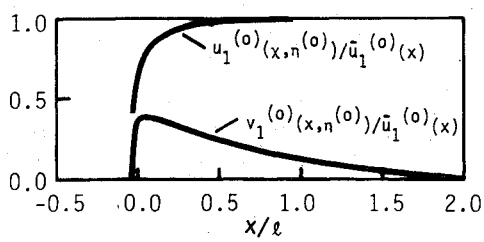

Fig. 6 Upstream velocities at the flame edge, $w_1/U_0 = 0.4$.

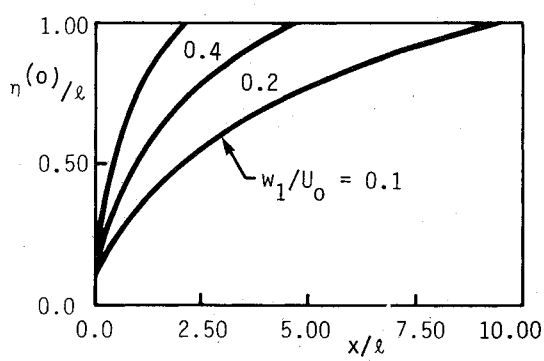

Fig. 7 Steady flame envelopes, $\lambda = 4.5$.

$$p_1^{(0)}(x) - p_2^{(0)}(x) = \rho_1(\lambda-1)w_1^2 \tag{54}$$

and

$$u_1^{(0)}(x,\eta^{(0)}) + v_1^{(0)}(x,\eta^{(0)})\frac{d\eta^{(0)}}{dx} = u_2^{(0)}(x,\eta^{(0)}) + v_2^{(0)}(x,\eta^{(0)})\frac{d\eta^{(0)}}{dx} \tag{55}$$

Differentiating Eq. (54) along the flame surface, we get [at $y = \eta^{(0)}(x)$],

$$\frac{\partial p_1}{\partial x} + \frac{\partial p_1}{\partial y}\frac{d\eta^{(0)}}{dx} = \frac{\partial p_2}{\partial x} + \frac{\partial p_2}{\partial y}\frac{d\eta^{(0)}}{dx} \tag{56}$$

Utilizing the momentum equations in region 2, we obtain

$$\frac{d^1 p_2}{dx} = -\rho_2\zeta_2^{(0)}\left(u_2^{(0)}\frac{d\eta^{(0)}}{dx} - v_2^{(0)}\right) - \rho_2\frac{d^1}{dx}\left[\frac{(u_2^{(0)})^2 + (v_2^{(0)})^2}{2}\right]$$

where

$$\frac{d^1}{dx} \equiv \left(\frac{\partial}{\partial x} + \frac{d\eta^{(0)}}{dx}\frac{\partial}{\partial y}\right)_{y=\eta^{(0)}(x)}$$

and

$$\zeta_2^{(0)}(x,\eta^{(0)}(x)) = \left(\frac{\partial v_2^{(0)}}{\partial x} - \frac{\partial u_2^{(0)}}{\partial y}\right)_{y=\eta^{(0)}(x)}$$

represent the vorticity produced by the steady flame.

Similarly, utilizing the momentum equations in region 1 and noting that the flowfield upstream of the flame is irrotational, we obtain from Eq. (56)

$$-\rho_1\frac{d^1}{dx}\left[\frac{(u_1^{(0)})^2 + (v_1^{(0)})^2}{2}\right] = -\rho_2\zeta_2^{(0)}\left[u_2^{(0)}\frac{d\eta^{(0)}}{dx} - v_2^{(0)}\right] - \rho_2\frac{d^1}{dx}\left[\frac{(u_2^{(0)})^2 + (v_2^{(0)})^2}{2}\right] \tag{57}$$

Utilizing the matching conditions, Eqs. (53) and (55), to obtain $u_2^{(0)}(x,\eta^{(0)})$ and $v_2^{(0)}(x,\eta^{(0)})$ in the above equation, we can express the vorticity produced by the flame as

$$\zeta_2^{(0)}(x,\eta^{(0)}) = \frac{-1}{2w_2\sec\Theta^{(0)}}\frac{d^1}{dx}\left[\left(u_1^{(0)} + v_1^{(0)}\frac{d\eta}{dx}\right)^2\cos^2\Theta^{(0)} - \lambda\{(u_1^{(0)})^2 + (v_1^{(0)})^2\}\right] \tag{58}$$

The above equation relates the vorticity generated by the flame with the flowfield upstream of the flame alone. This gives the source term in the Poisson equation of the streamfunction for the downstream flow. The upstream flowfield is known exactly from the representation of Sec. III.B. For plane flames, $d\eta^{(0)}/dx = \text{constant}$ $v_1^{(0)} = 0$, and $u_1^{(0)} = w_1\operatorname{cosec}\Theta^{(0)}$, and from Eq. (58) we notice that there is no vorticity produced by the steady plane flames.

IV. Time-Dependent Flame Calculations

Consider now the time-dependent counterpart to the steady analysis (Sec. III.C) of the integral relations. With the assumed decomposition [Eqs. (42)] of the dependent

variables in the integral relations Eqs. (17-20), we obtain the following governing equations for the nonsteady variables. Only the linear terms in the perturbation quantities are retained. The axial velocity perturbations at the flame surface can be written as

$$u_1^{(1)}(x,\eta,t) = \frac{\partial u_1^{(0)}}{\partial y}(x,\eta^{(0)})\eta^{(1)}(x,t) + u_1^{(1)}(x,\eta^{(0)},t) \quad (59)$$

$$u_2^{(1)}(x,\eta,t) = u_1^{(1)}(x,\eta,t) + w_1(\lambda-1)\cos^3\Theta^{(0)}\frac{\partial \eta^{(1)}}{\partial x} \quad (60)$$

In region 1, the continuity equation is

$$\frac{\partial \eta^{(1)}}{\partial t} + (\bar{u}_1^{(0)} - w_1\sin\Theta^{(0)})\frac{\partial \eta^{(1)}}{\partial x} + \frac{d\bar{u}_1^{(0)}}{dx}\eta^{(1)} + \frac{d\eta^{(0)}}{dx}\bar{u}_1^{(1)} - (\ell-\eta^{(0)})\frac{\partial \bar{u}_1^{(1)}}{\partial x} = 0 \quad (61)$$

and the x-momentum equation is

$$\frac{\partial \bar{u}_1^{(1)}}{\partial t} + \bar{u}_1^{(0)}\frac{\partial \bar{u}_1^{(1)}}{\partial x} + \frac{d\bar{u}_1^{(0)}}{dx}\bar{u}_1^{(1)} + \frac{1}{\rho_1}\frac{\partial \bar{p}_1^{(1)}}{\partial x} + \frac{w_1\sec\Theta^{(0)}}{\ell-\eta^{(0)}}[u_1^{(1)}(x,\eta^{(0)},t) + \frac{\partial u_1^{(0)}}{\partial y}(x,\eta^{(0)})\eta^{(1)} - \bar{u}_1^{(1)}] + \frac{w_1}{\ell-\eta^{(0)}}[u_1^{(0)}(x,\eta^{(0)}) - \bar{u}_1^{(0)}] \times \left[\sin\Theta^{(0)}\frac{\partial \eta^{(1)}}{\partial x} + \frac{\sec\Theta^{(0)}\eta^{(1)}}{\ell-\eta^{(0)}}\right] = 0 \quad (62)$$

In region 2, the continuity equation is

$$\frac{\partial \eta^{(1)}}{\partial t} + (\bar{u}_2^{(0)} - w_2\sin\Theta^{(0)})\frac{\partial \eta^{(1)}}{\partial x} + \frac{d\bar{u}_2^{(0)}}{dx}\eta^{(1)} + \frac{d\eta^{(0)}}{dx}\bar{u}_2^{(1)} + \eta^{(0)}\frac{\partial \bar{u}_2^{(1)}}{\partial x} = 0 \quad (63)$$

and the x-momentum equation is

$$\frac{\partial \bar{u}_2^{(1)}}{\partial t} + \bar{u}_2^{(0)}\frac{\partial \bar{u}_2^{(1)}}{\partial x} + \frac{d\bar{u}_2^{(0)}}{dx}\bar{u}_2^{(1)} + \frac{1}{\rho_2}\frac{\partial \bar{p}_2^{(1)}}{\partial x} + \frac{w_2\sec\Theta^{(0)}}{\eta^{(0)}}\left[\bar{u}_2^{(1)} - u_1^{(1)}(x,\eta^{(0)},t) - \frac{\partial u_1^{(0)}}{\partial y}(x,\eta^{(0)})\eta^{(1)} - w_1(\lambda-1)\cos^3\Theta^{(0)}\frac{\partial \eta^{(1)}}{\partial x}\right] + \frac{w_2}{\eta^{(0)}}[\bar{u}_2^{(0)} - u_1^{(0)}(x,\eta^{(0)}) - w_1(\lambda-1)\sin\Theta^{(0)}]\left[\sin\Theta^{(0)}\frac{\partial \eta^{(1)}}{\partial x} - \frac{\sec\Theta^{(0)}\eta^{(1)}}{\eta^{(0)}}\right] = 0 \quad (64)$$

The zeroth-order solution, which describes the steady flame development, is discussed in Sec. III.C. It provides the steady-state variables in the above system of differential equations for the perturbation quantities.

The normal momentum balance across the flame [Eq. (6)] states that the pressure perturbation is continuous across the flame.

$$\bar{p}_1^{(1)}(x,t) = \bar{p}_2^{(1)}(x,t) \quad (65)$$

The steady axial velocity at the upstream flame edge, $u_1^{(0)}(x,\eta^{(0)})$, is approximated by Eq. (41). In addition, we assume

$$u_1^{(1)}(x,\eta^{(0)},t) = \bar{u}_1^{(1)}(x,t) \quad (66)$$

Validity of the above approximation is verified by generating the nonsteady flame envelopes with a time-dependent source flow. The technique is very similar to the steady flow representation of Sec. III.B.

We consider the flame region to be excited by a harmonic pressure wave with wave number κ_2^- from the downstream direction. This generates a transmitted wave of wave number κ_1^- upstream of the flame and a reflected wave of wave number κ_2^+ downstream of the flame. Let the transmitted wave upstream of the flame be represented by

$$\frac{\bar{p}_1^{(1)}}{\gamma p_0} = P_1^- \exp[-i(\omega t + \kappa_1^- x)] \quad (67)$$

Since there is no acoustic wave incident on the flame zone from the upstream direction, we can write the associated velocity perturbation upstream of the flame region as

$$\frac{\bar{u}_1^{(1)}}{C_1} = -P_1^- \exp[-i(\omega t + \kappa_1^- x)] \quad (68)$$

This gives the boundary conditions at $x=0$ for the pressure and velocity perturbations as

$$\frac{\bar{p}_1^{(1)}}{\gamma p_0}(x=0,t) = P_1^- e^{-i\omega t} \quad (69)$$

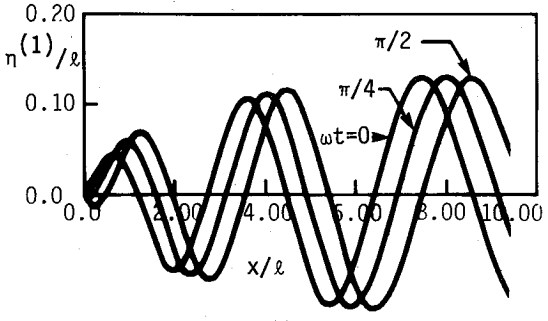

Fig. 8 Nonsteady flame perturbations.

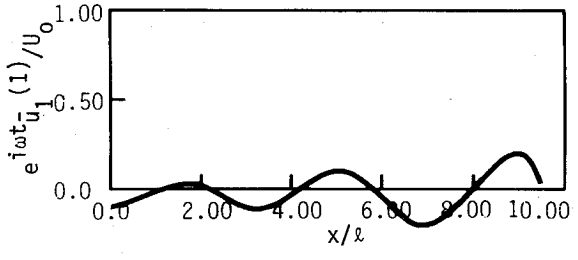

Fig. 9 Velocity perturbation upstream of the flame.

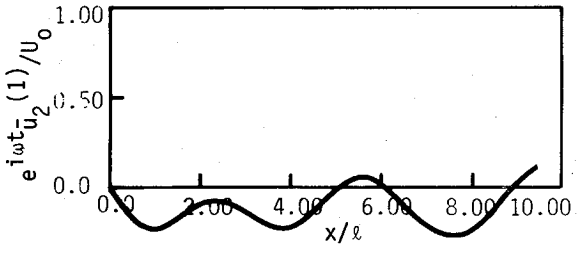

Fig. 10 Velocity perturbation downstream of the flame.

$$\frac{\tilde{u}_1^{(I)}}{C_1}(x=0,t) = -P_I^- e^{-i\omega t} \tag{70}$$

The flame is attached to the flame holder at $x=0$,

$$\eta^{(I)}(x=0,t) = 0 \tag{71}$$

Velocity perturbation downstream of the flame holder is assumed to be zero,

$$\tilde{u}_2^{(I)}(x=0,t) = 0 \tag{72}$$

It should, however, be noted that in the present integral formulation, the flame development adjacent to the flame holder is not represented accurately. Detailed calculations near the flame holder should take into account the viscous and heat conduction effects. Present calculations indicated that the flame response is rather insensitive to the choice of $\tilde{u}_2^{(I)}(0,t)$, suggesting that the behavior of the nonsteady wake downstream of the flame holder may not be of dominant influence on the nonsteady flame development.

V. Results and Discussion

As can be seen from Sec. III.A, the principal parameters that affect the steady flame development are the upstream translational speed U_0, duct width 2ℓ, flame speed w_1/U_0, and the density ratio across the flame $\lambda=\rho_1/\rho_2$. For the nonsteady response of the flame region, the radian frequency ω of the disturbance is an additional important parameter. We utilize the reduced frequency $\Omega=\omega\ell/U_0$ to evaluate the burner response.

A flame speed of $w_1/U_0=0.1$, density ratio $\lambda=4.5$, approach Mach number $M_0=0.1$, and reduced frequency $\omega\ell/U_0=3.66$, are chosen to describe the burner operation for the results presented here.

Figure 8 shows the nonsteady flame envelopes for the above operating conditions of the burner. The flame envelopes are shown for three different time intervals given by $\omega t=0$, $\pi/4$, and $\pi/2$. The velocity perturbations, real parts of $e^{+i\omega t}\tilde{u}_1^{(I)}/U_0$, and $e^{+i\omega t}\tilde{u}_2^{(I)}/U_0$, are shown in Figs. 9 and 10. The perturbation quantities shown in Figs. 8-10 are the responses for an acoustic disturbance of reduced frequency $\Omega=3.66$ incident on the flame region from downstream. The flame perturbation exhibits a traveling wave pattern with considerable amplification in the downstream direction. This has to be differentiated from the classical Landau instability of plane flames, wherein the flame perturbation is stationary, with no associated phase speed.

For the present case of the confined stabilized flame, there is vorticity production by the steady flame due to the curvature of the flame. This vorticity production by the flame can be calculated from the flame shape and the upstream irrotational flowfield as shown in Sec. III.D. A possible mechanism to explain the calculated growth of the disturbance in the flame region is the amplification of the shed vorticity, which behaves as an unstable shear layer. This aspect was explored in some detail. In the case of plane flames, there is no vorticity production by the steady flame. The growth rate and phase speed obtained from a local analysis[19] of the stability of the flame sheet, modeled as an interface separating the two regions with velocities $\tilde{u}_1^{(0)}(x)$ and $\tilde{u}_2^{(0)}(x)$ are in general agreement with the nonsteady flame calculations presented here.

The velocity and pressure perturbations enable us to obtain the acoustic transmission and reflection properties of the flame region. The response spectra[19] of the flame region show active response, and at certain well-defined frequencies there is a strong amplification of an input disturbance. These energetic modes occur at reduced frequencies $\omega L/\bar{\sigma}=3\pi/2$, $7\pi/2$, etc. (where $\bar{\sigma}$ is the average phase speed of the flame perturbation), and are distinguished by the manner in which they fit into the end conditions of the flame at the flame holder and at the duct wall.

In a practical combustion system like the aircraft afterburner or the utility boiler, these burner characteristics couple the nonsteady flame response with the acoustics of the combustion chamber. A typical application to a rudimentary afterburner was discussed by Marble et al.[18]

Acknowledgments

The author is most grateful to Prof. Frank Marble for his scholarly guidance and generous support during this investigation. The many stimulating discussions the author had with Dr. Sebastien Candel are greatly appreciated. The work was supported in part by the U.S. Department of Energy, Grant EX-76-G-03-1305.

References

[1]Emmons, H. W., ed., *Fundamentals of Gas Dynamics, High Speed Aerodynamics and Jet Propulsion,* Vol. III, Princeton University Press, Princeton, N. J., 1958, p. 611.

[2]Scurlock, A. C., "Flame Stabilization and Propagation in High-Velocity Gas Streams," MIT, Cambridge, Mass., Meteor Report No. 19, 1948.

[3]Tsien, H. S., "Influence of Flame Front on the Flow Field," *Journal of Applied Mechanics,* Vol. 73, June 1951, pp. 188-194.

[4]Ball, G. A., "Combustion Aerodynamics. A Study of a Two-Dimensional Flame," Dept. of Engineering Science and Applied Physics, Harvard University, Cambridge, Mass., July 1951.

[5]Fabri, J., Siestrunck, R., and Foure, C., "On the Aerodynamic Field of Stabilized Flames," *Fourth Symposium (International) on Combustion,* The Williams and Wilkins Company, Baltimore, 1953, pp. 443-450.

[6]Iida, H., "Combustion in Turbulent Gas Streams," *Sixth Symposium (International) on Combustion,* Reinhold Publishing Corp., New York, 1956, pp. 341-350.

[7]Williams, G. C., Hottel, H. C., and Scurlock, A. C., "Flame Stabilization and Propagation in High Velocity Gas Streams," *Third Symposium on Combustion and Flame and Explosion Phenomena,* The Williams and Wilkins Co., Baltimore, Md., 1949, pp. 21-40.

[8]Thurston, D. W., "An Experimental Investigation of Flame Spreading from Bluff Body Flameholders," Engineer's Thesis, California Institute of Technology, Pasadena, Calif., 1958.

[9]Wright, F. H. and Zukoski, E. E., "Flame Spreading from Bluff Body Flame Holders," *Proceedings, Eighth Symposium (International) on Combustion,* The Williams and Wilkins Co., Baltimore, Md., 1960, pp. 933-943.

[10]Zukoski, E., "Afterburners," *The Aerothermodynamics of Aircraft Gas Turbine Engines,* edited by G. C. Oates, AFAPL-TR-78-52, 1978, Chap. 21.

[11]Landau, L., "On the Theory of Slow Combustion," *Acta Physicochimicca U.R.S.S., L.,* Vol. XIX, No. 1, 1944, pp. 77-85.

[12]Markstein, G. H., "Experimental and Theoretical Studies of Flame-Front Stability," *Journal of Aeronautical Sciences,* Vol. 18, 1951, pp. 199-209.

[13]Istratov, A. G. and Librovich, V. V., "Stability of Flames," Army Foreign Science and Technology Center, Washington, D. C., FSTC-23-952-68, 1969.

[14]Petersen, R. E. and Emmons, H. W., "Stability of Laminar Flames," *Physics of Fluids,* Vol. 4, No. 4, 1961, pp. 456-464.

[15]Blackshear Jr., P. L., "Growth of Disturbances in a Flame Generated Shear Region," NACA 3830, Nov. 1956.

[16]Marble, F. E. and Candel, S. M., "An Analytical Study of the Non-Steady Behavior of Large Combustors," *Seventeenth Symposium (International) on Combustion,* The Combustion Institute, Pittsburg, Aug. 1978, pp. 761-769.

[17]Le Chatelier, C. and Candel, S. M., "Flame Spreading in Compressible Duct Flow," *Proceedings of First International Specialists Meeting of the Combustion Institute,* Bordeaux, France, July 1981.

[18]Marble, F. E., Subbaiah, M. V., and Candel, S. M., "Analysis of Low-Frequency Disturbances in Afterburners," *Proceedings, Specialists Meeting on Combustion Modeling,* AGARD Propulsion and Energetics Panel, Cologne, AGARD-CP-275, Oct. 1979, pp. 17.1-17.11.

[19]Subbaiah, M. V., "Non-Steady Behavior of a Flame Spreading from a Point in a Two-Dimensional Duct," Ph.D. Thesis, California Institute of Technology, Pasadena, Calif., 1980.